Numerical Validation of the Experimental Cyclic Response of RC Frames

M.T. Braz-Cesar[1], D.V. Oliveira[2] and R.C. Barros[3]
[1]Department of Applied Mechanics
Polytechnic Institute of Bragança, Portugal
[2]ISISE – Department of Civil Engineering
University of Minho, Portugal
[3]FEUP – Department of Civil Engineering
Faculty of Engineering of the University of Porto, Porto, Portugal

Abstract

In this paper is estimated the numerical cyclic response of RC frames with and without masonry infill's through a simplified nonlinear analysis using a commercial finite element method (FEM) package. The numerical model is based on the experiments carried out in the National Laboratory of Civil Engineering (LNEC) and the numerical and experimental results are compared to assess the accuracy of the simplified analysis for the bare frame and for the infill frame. To take into account the highly nonlinear behaviour of reinforced concrete (RC) frames due to large deformations, a numerical model based on the inelastic hinge method is used with a higher complexity of the hinge constitutive laws, which allows verifying the suitability of every hinge model to the experimental results.

Keywords: infill RC frames, cyclic response of RC frames, nonlinear analysis.

1 Introduction

The widespread buildings constructed in Portugal and also in other European countries present a well-known structural solution based in the spatial repetition of masonry infill frames. The damage and collapse of structures of this type, as a result of significant floor lateral deformations induced by moderate to severe seismic events, are nowadays two of the main concerns of the structural designers.
For seismic design a spectral response procedure is normally used allowing the verification of the resistant capacity and serviceability limits. These verifications guarantee the resistant capacity necessary to prevent the structure collapse and enough stiffness to prevent an excessive deformation with the consequent reduction of damage and a better use of the building during the seismic event. In these methodologies the response depends on the structure ductility that involves the reduction of the seismic efforts through ductility coefficients to simulate the nonlinear behaviour when an elastic analysis is implicated in the design.

This methodology is based on the capacity of the structural elements to accommodate plastic deformations (nonlinear behaviour) without compromising the structure stability. However, the new analysis and design methodologies allow to define the criteria that manage the structural response for some levels of structural performance and therefore to identify some levels of damage for a severe earthquake. On the other hand, these design philosophies start to be implemented in computation tools, namely those based on the Finite Element Method (FEM) that implies the validation requirement of the software implicit codes. On this context, the main purpose of this paper is to validate some simplified nonlinear models used to carry out a material nonlinear analysis. This simplified analysis is based on the definition of critical sections of the bar elements with inelastic behaviour, and on the constitutive models for each critical section, with increasing complexity in characterizing the RC frame damage level. To validate the nonlinear model, available experimental information carried out in the National Laboratory of Civil Engineering (LNEC) was used.

2 Experimental results

In the scope of an experimental research program developed at LNEC to study the influence of brick masonry panels on cyclic response of RC frames, a bare frame and several infill frames were tested (Pires [1]). A constant vertical load (P= 100 kN) at the top of each column and a lateral increasing cyclical load/displacement pattern at the beam level were applied. The main characteristics of the RC frame used in this study and the cyclic law are shown in Figure 1.

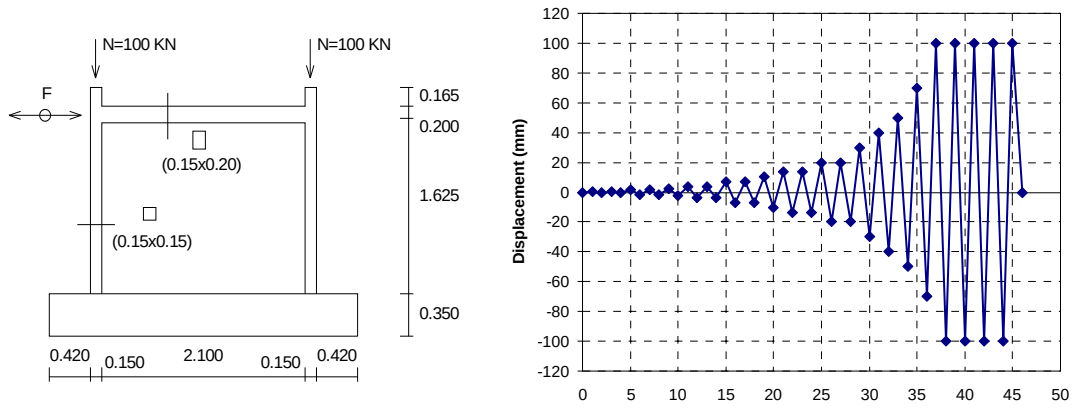

a) b)

Figure 1: Experimental frame: a) general description; b) lateral displacement law.

The mechanical characteristics, of the materials used in the RC bare frame, are: C20/25 concrete; S400 for longitudinal reinforcement and S500 for the stirrups. To guarantee a good concrete confinement at the critical sections at the near end of each element a narrow stirrup spacing was used (Ø4//0.05 instead of general Ø4//0.10) as shown in Figure 2.

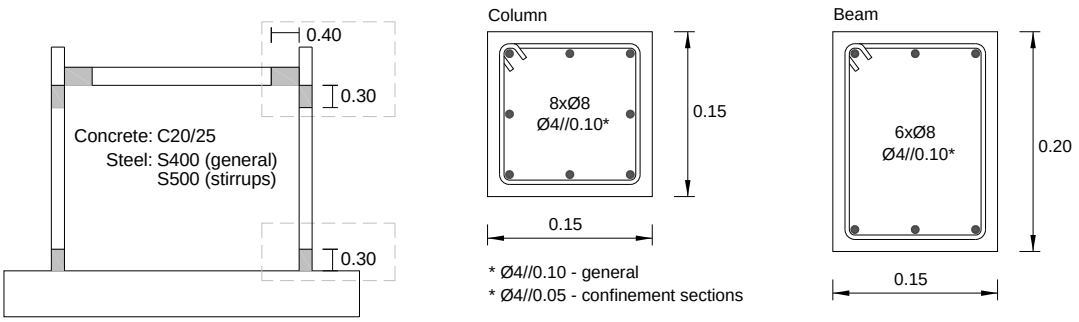

a) b)

Figure 2: RC frame: a) confinement sections; b) cross sections.

For the infill frames regular hollow brick masonry (30x20x15) was used. However, in the LNEC study [1], several experimental units were analysed to realize the influence of bond interface between the bare frame and the masonry. In this paper an unbounded infill setup was considered which best represents the real sequence of such buildings construction. Figure 3 indicates the experimental force-displacement cyclic results for the bare frame and for the infill frame.

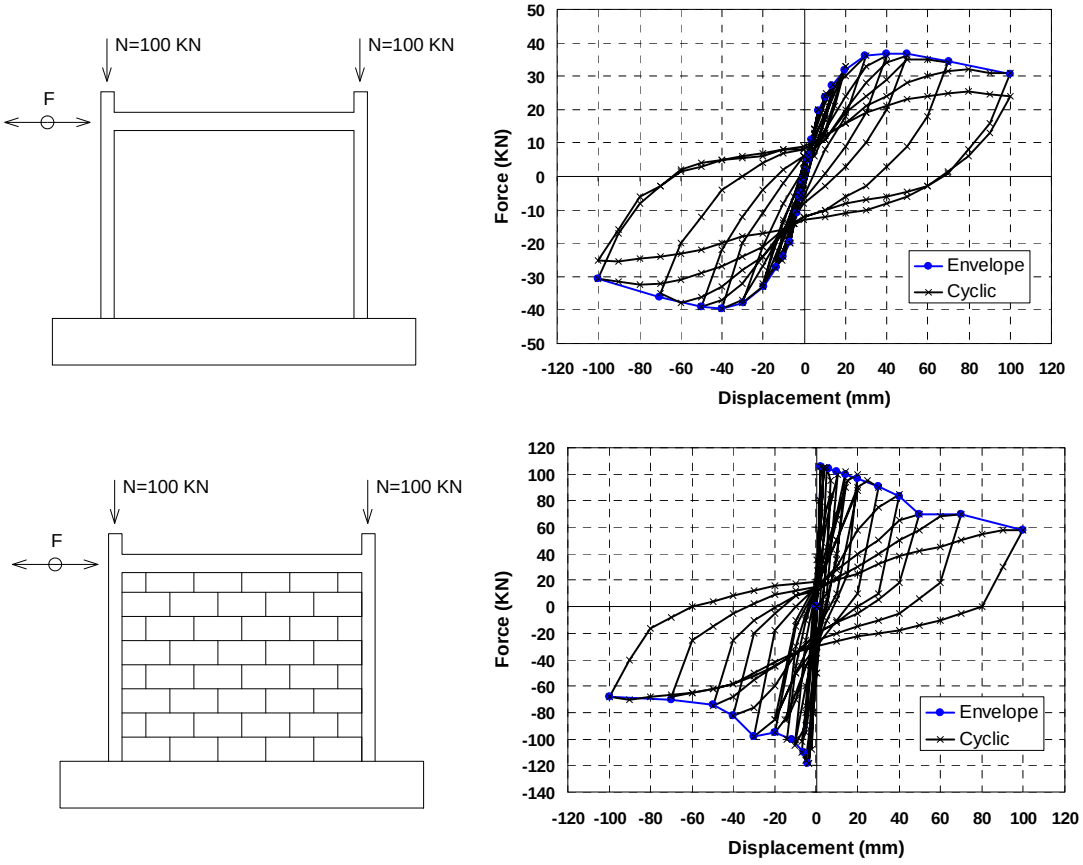

Figure 3: Experimental cyclic responses, respectively for bare and infill frames.

As it can be seen in this graphical representation an important incursion in the nonlinear regime is observed specially in the infill frame. The bare frame shows a smooth evolution with a maximum obtained just before the complete concrete cracking at the top and bottom columns ends (inelastic hinge configuration). After this point a soft stiffness decrease occurs without collapse but with significant column damage and inelastic spread of hinge effects.
The infill frame exhibits a well-known behaviour for this type of building solution with three branches that correspond to several distinct behaviours: an upward linear branch in which the RC frame and the infill masonry work as one building block until the masonry cracking starts; an upward nonlinear branch related with the masonry cracking and a decreasing nonlinear branch related with the damage of the infill panel. The test was stopped with a fragile column rupture due to shear, that was observed during the last cycle occurrence.

3 Numerical model of RC frame without infill

Aiming at the numeric validation of the experimental results presented previously, the framed structure was modelled resorting to beam elements, for which different nonlinear constitutive laws were adopted to assess the building performance. The structural model, the different constitutive laws as well as the main numerical results, will be presented in this section.
Framed structures, when subjected to cyclic loads, usually present a structural behaviour characterized by the development of plastic hinges at the extremities of the elements (Figure 4a). As it would be expected, the experimental results to be modelled here show clearly this behaviour.

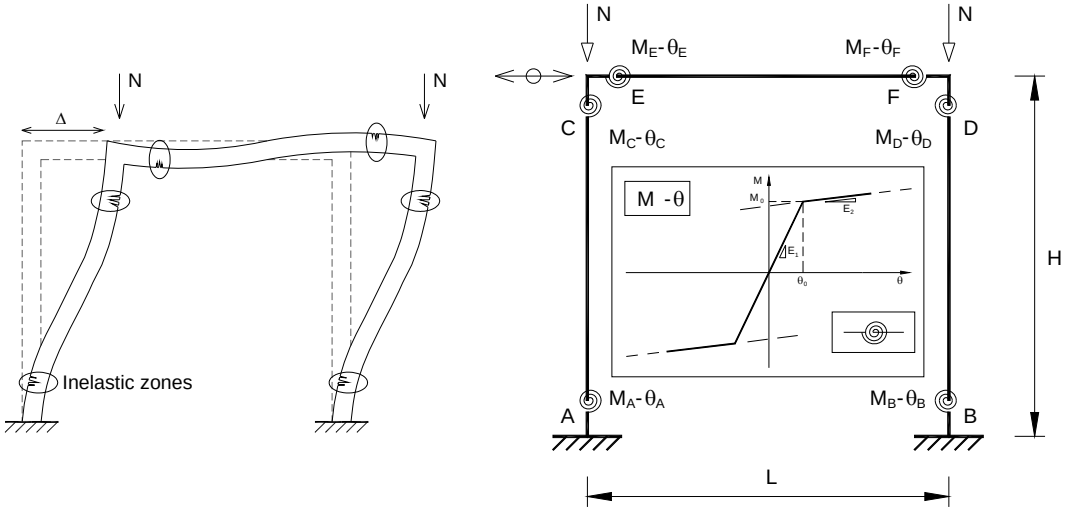

a) Frame critical sections b) Idealized plastic hinges.

Figure 4: Typical critical zones in framed structures.

The typical formation of plastic hinges in specific zones has promoted the development of several methodologies that allow accomplishing nonlinear analyses of framed structures (both static and dynamic) in a non-complex fashion.
This type of behaviour led to the implementation of computational hinge-like models in commercial packages for the automatic computation of structures. The software used in the present work, MIDAS\Civil [2], is a good example of the integration of these methodologies into an algorithm based on the FEM. In this context, the validation of this commercial software and its associated calculation procedures constitutes also one of the purposes to be achieved in this research work.
Basically, these methodologies are founded on the simplification associated to the concentration of the nonlinear behaviour in zones in correspondence with the development of plastic hinges (Fardis and Panagiotakos [3]).
Therefore, the first step consists in the location of these critical zones that, in the case of framed structures subjected to horizontal loads, are usually located at the extremities of the elements (Figure 4b). The following step corresponds to the definition of the constitutive law that rules the formation and further development of the plastic hinge. Its definition is of critical importance as it is not possible to know in advance the best law to be used. Naturally, experimental results have a fundamental role in the definition and validation of constitutive laws to be used.
The software employed in this work makes use of two different procedures to define the nonlinear seismic behaviour of RC framed structures (Paulay and Priestley [4]), namely: Plastic hinge model (PHM) and Fiber model (FM). The main difference between the two models lies in the way the constitutive laws are defined and used.
In the case of PHM an envelope curve, that represents the global behaviour of the entire cross section in terms of bending moment-curvature, is defined; in the case of FM it is necessary to establish constitutive laws associated to the axial deformation of each of the materials (or fibers) that compose the section.
Within the PHM, the modelling of the plastic hinges is done through the insertion of a zero-length element connecting two adjacent beam elements (Figure 5a), for which a constitutive law has to be defined in each of the six degrees of freedom.

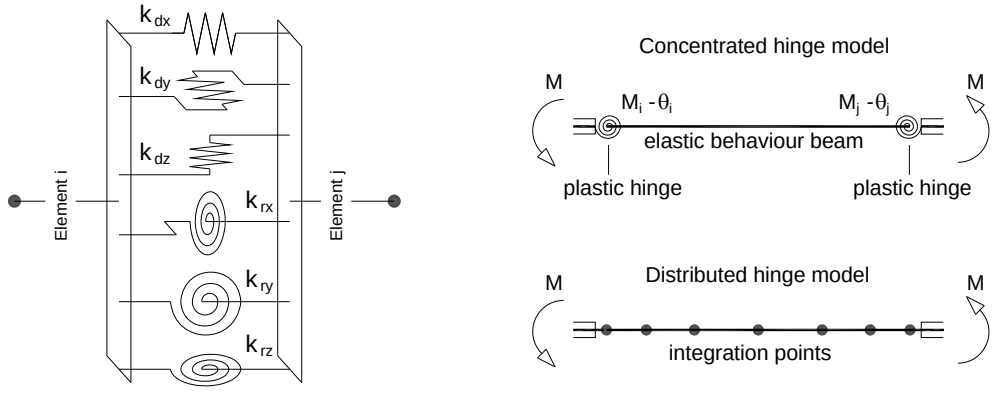

a) Components of the zero-length element (plastic hinge).

b) Plastic hinges in a beam element.

Figure 5: Idealized plastic hinges.

According to the MIDAS software's manual [2], it is possible to consider three different types of plastic hinges within the PHM, as follows: concentrated hinges, distributed hinges and spring-like hinges. The former two types are related to the modelling of the nonlinear behaviour in beam elements, whereas the last type is associated with the modelling of nonlinear phenomena in boundary elements.
Figure 5b represents the structural model associated to the use of concentrated and distributed plastic hinges. The mathematical formulation results from the application of the flexibility method and the hinges are defined through the use of force-displacement and bending moment-curvature relationships.

Within the concentrated hinge concept, the nonlinear behaviour is obtained through the introduction of zero-length translation and rotation springs located at the ends or at the centre of the beam element. The remaining parts of the element perform always in an elastic fashion.
For the distributed hinge concept, integration points up to a maximum of twenty have to be defined. Their location is determined by their number and the distance between two integration points decreases as the beam extremities approach. Therefore, the use of the distributed hinge concept allows, in general, a better representation of reality, however, computation becomes more time consuming.

Another important aspect is related with the attainment of yielding of the materials that compose the cross section. In the case of reinforced concrete beams submitted to bending moments (Figure 6), yielding is associated with two main features: appearance of the first crack (bending moment M_{cr}) and yielding of the most compressed concrete fibre (it is assumed that the steel remains elastic).

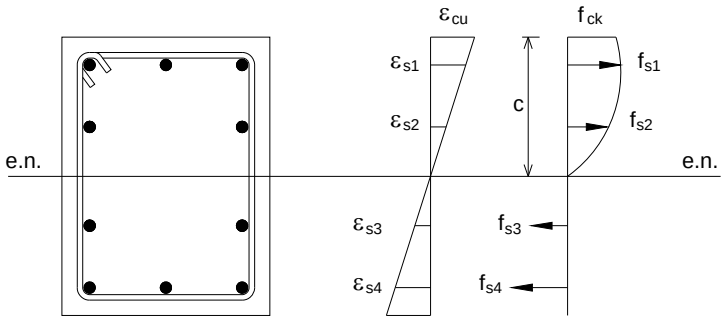

Figure 6: Yielding in reinforced concrete beam elements.

Independent hinges are to be defined for each of the degrees of freedom. When the applied load is reversible and variable in time, as it is the case of the load under analysis, the constitutive laws used to model the structural behaviour must also incorporate hysteretic properties associated to the unloading-reloading processes.
The hysteretic models included in the software are defined through an envelope curve and are grouped as follows: simplified models; models with stiffness degradation; nonlinear elastic models and models with slipping effects. The laws established for these groups allow adopting different types of material behaviour:

hardening model; secant unloading/loading model; Clough's model; tri-linear degradation and Takeda's models. Except for the Clough's model, the other models are in essence based on tri-linear monotonic laws.

In this work, three different models related with concentrated and distributed plastic hinges were considered, with increasing degree of complexity: bilinear Clough's model; tri-linear Takeda's model and tetra-linear Takeda's model (Cesar, Oliveira and Barros: [5], [6], [7]). Notice that a good numerical model must be able to catch conveniently the section element behaviour and the global behaviour as well. To accomplish this, the model must employ the following characteristics: stiffness decrease due to deformation; stiffness decrease in the unload path; resistance decrease; P-Δ effect; influence of shear force effect (pinching), the bond deterioration and the reinforcement slipping (slipping). Therefore, this study is also intended to verify if the models can perform a good numerical approach.

The first model (Clough's model) corresponds to a simplified constitutive relationship based on a bilinear variation of stiffness (Figure 7).

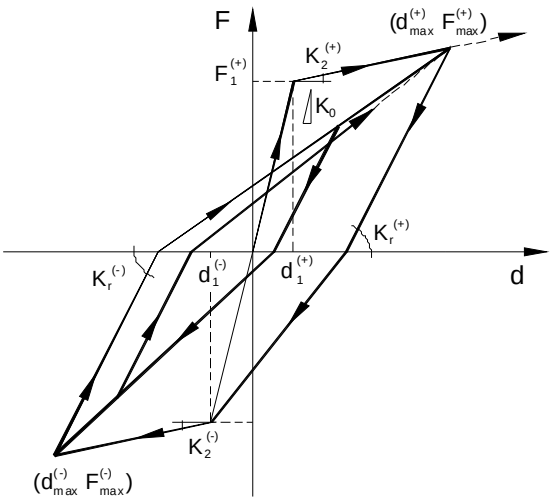

Figure 7: Idealized Clough's Plastic hinge model.

The unloading stiffness is obtained from a reduction of the elastic stiffness according to the following equation:

$$K_R = K_0 \cdot \left| \frac{D_y}{D_m} \right|^{\beta} \leq K_0 \tag{1}$$

where K_0 is the elastic stiffness, K_R is the unloading stiffness, D_y is the yielding displacement associated to load reversal, D_m is the maximum displacement associated to load reversal and β is a parameter involved in the definition of the unloading stiffness.

The Clough's model is based on the following procedure:

(i) If a load reversal happens, then the load point moves towards the opposite maximum displacement; (ii) If yielding has not happen yet, the load point moves in the direction of the yield displacement of the envelope curve;

(ii) The procedure should be started with the establishment of the envelope constitutive law. The geometric properties of the sections where plastic hinges are expected to occur are represented in figure 2b.

For the computation of the constitutive M-θ laws associated to each section, the BIAX algorithm (Wallace [8]) was used, which allows one to obtain the capacity curve in terms of bending moment of a reinforced concrete cross section. Based on the mechanical characteristics of the materials used in the experiments and knowing that columns are subjected to a compressive load of 100 kN, it was possible to compute the M-θ capacity curves of beams and columns, as illustrated in Figure 8.

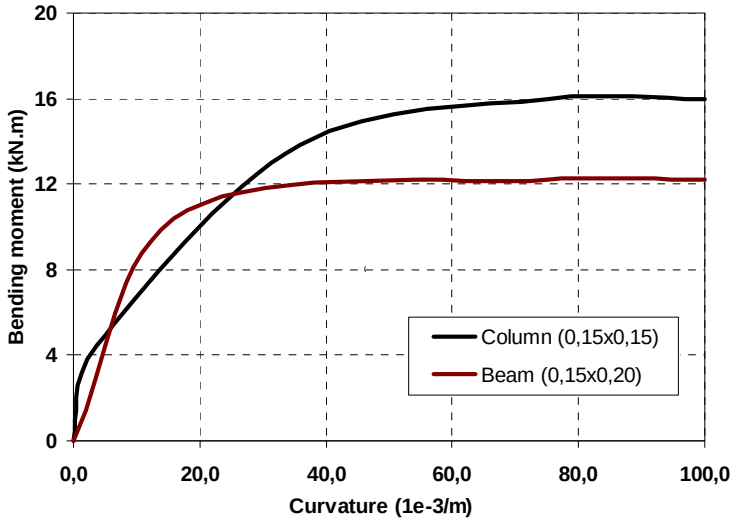

Figure 8: Bending moment-curvature diagrams of both column and beam elements.

The column capacity curve shows an almost tetralinear development while the capacity curve of the beam presents a development essentially trilinear. The application of the Clough's model to these curves implies a simplification because only bilinear curves are possible within this model (Figure 9).
The inclusion of these curves requires the knowledge of both the elastic and cracked stiffness, which can be obtained directly from the BIAX software (Wallace [8]). The parameters used in this study are shown in Table 1.

Table 1 – Elastic and reduced stiffness (Clough´s model).

	Column	Beam
K_0	1380 kNm^2	610 kNm^2
K_1	6.9 (0.05%)	30.5 (20%)

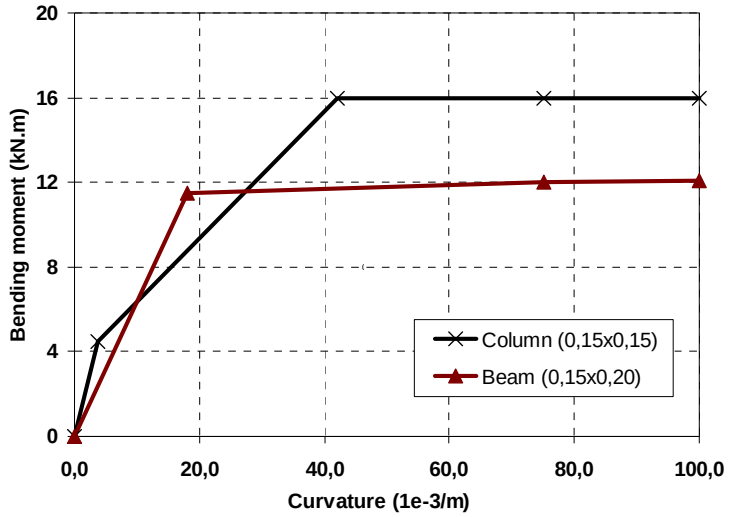

Figure 9: Idealized bending moment-curvature diagrams.

Using these parameters and performing a fitting of the unloading stiffness, it was possible to obtain the structural load-displacement curve represented in Figure 10.

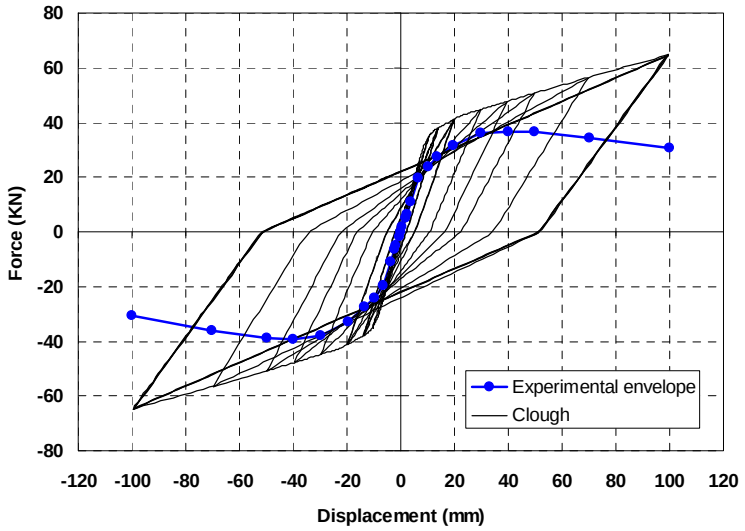

Figure 10: Load-displacement curve (Clough's model).

Comparing this curve against the experimental results, it is clear that the model does not represent adequately the real behaviour of the structure, where a significant increase of the strength is visible mainly for high lateral displacements. It is clear that these differences are directly linked to simplifications related to the bilinear law.

Next, the structure was modelled using a tri-linear envelope law (tri-linear Takeda´s model), that allows a more powerful representation of the structural behaviour of the cross section (Figure 11).

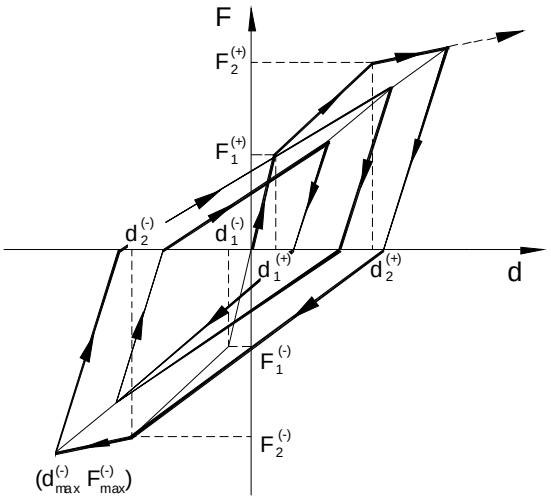

Figure 11: Constitutive law of the tri-linear Takeda's model.

Within this model, the development of two internal cycles or loops under reversal loads is now possible. Following a load reversal, the external loop occurs if the target point has been reached whereas the internal loop develops before reaching the target point.
Within the external loop, the unloading stiffness computation is based on the location of the load reversal point only. This unloading stiffness is obtained through the following equation:

$$K_{R0} = \left\{ \frac{F_y + F_c}{D_y + D_c} \right\} \cdot \left(\frac{D_y}{D_c} \right)^{\beta} \tag{2}$$

where K_{R0} represents the unloading stiffness of the external loop, F_c and D_c are the load and displacement associated to the first occurrence of yielding opposite to the load reversal point, F_y and D_y are the load and displacement associated to the second occurrence of yielding opposite to the load reversal point, D_m is the maximum displacement opposite to the load reversal point and β is a parameter used to compute the unloading stiffness of the external loop.
If the current load goes from positive to negative or vice-versa, the load point moves towards the maximum displacement. If yielding has not happen before, there is no change of the reloading stiffness.
In the case of the internal loop, the equation that controls unloading is given by the following equation:

$$K_{Ri} = \gamma \cdot K_{R0} \tag{3}$$

where K_{Ri} represents the unloading stiffness of the internal loop, K_{R0} is the unloading stiffness of the external loop where the load reversal point stands and γ is a reduction parameter.

Figures 12 and 13 illustrate the different possibilities involved in the formation of the hysteretic curves.

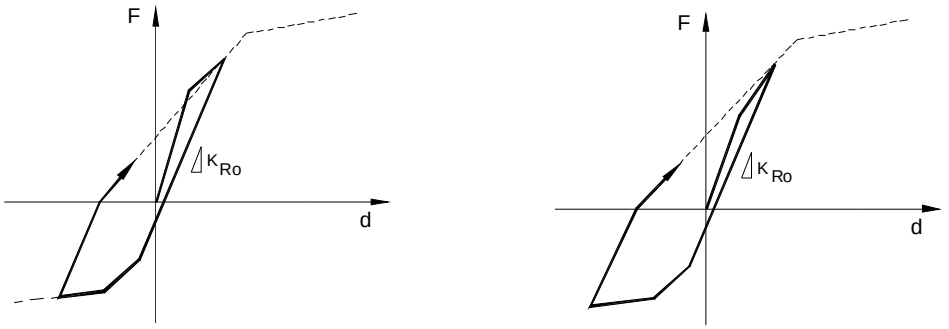

Figure 12: Unloading prior to yielding (tri-linear Takeda's model).

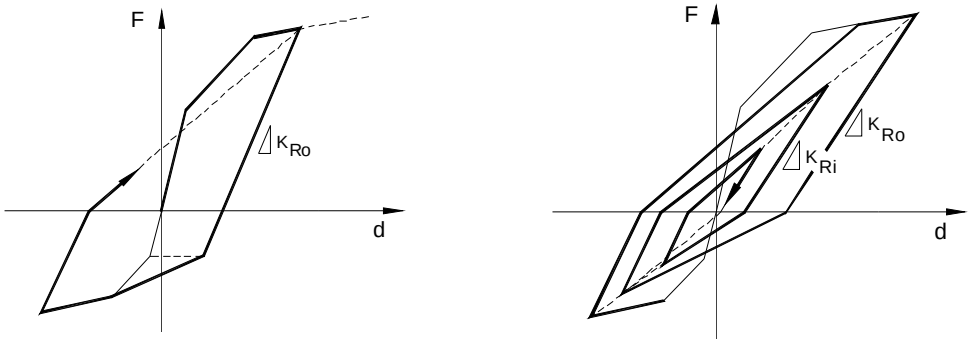

a) Unloading subsequent to yielding. b) Different allowable internal loops.

Figure 13: Unloading after yielding (tri-linear Takeda's model).

The monotonic stiffness values considered within this second constitutive model are represented in Table 2.

Table 2 – Elastic and reduced stiffness (tri-linear Takeda's model).

	Column	Beam
K_0	1380 kNm^2	610 kNm^2
K_1	276 (20%)	30.5 (5%)
K_2	6.9 (0.5%)	-

Based on these values and performing a fitting of the unloading stiffness parameters (it was adopted 0.75 for the exponent in unloading stiffness calculation and 1.00 for the inner loop unloading stiffness calculation), the obtained load-displacement curve is illustrated in Figure 14.

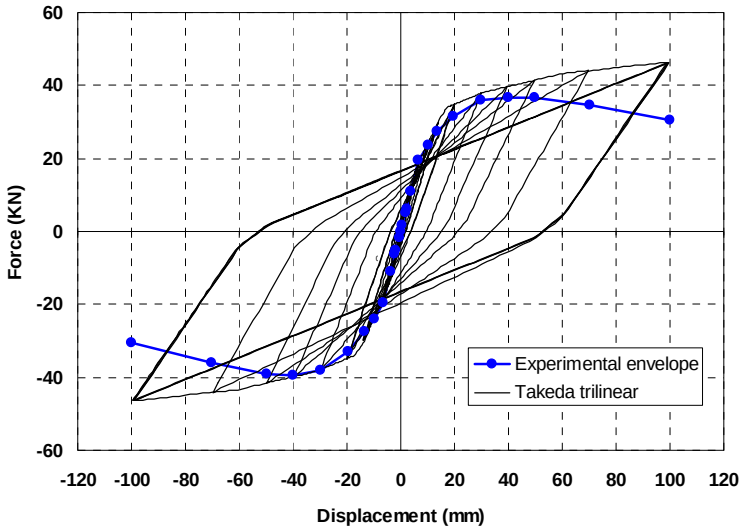

Figure 14: Load-displacement curve (tri-linear Takeda's model).

When compared with the model of Clough, this second model represents the experimental behaviour of the structure in a better way. The initial part of the load-displacement curve shows a good resemblance of the experimental and numerical results. The numerical hysteretic loops show a smooth variation of stiffness, but not in total agreement with the experimental results.

As happened before with the simplest model, an increase of strength with increasing lateral displacements was observed, although here this increase was not so significant as before.

The two aforementioned models (Clough's bilinear and Takeda's tri-linear) do not consider the possibility of a softening behaviour (negative stiffness), which most probably would allow to better approximate the numerical behaviour of the structure to experimental results. Therefore, a strength increase with increasing lateral displacement is observed in both models.

The tetra-linear Takeda's model, originated by a modification of the tri-linear Takeda's model through the inclusion of a fourth descending branch (with a softening negative stiffness symmetric of the last ascending positive stiffness), allows surpassing the aforementioned problem. Its unloading-reloading rules remain similar to the ones presented for the tri-linear model.

Figure 15 illustrates the typical hysteric curves (both external and internal ones) of the tetra-linear model. Table 3 shows the monotonic stiffness values adopted for the simulation of the experimental results.

Table 3 – Elastic and reduced stiffness (tetra-linear Takeda's model).

	Column	Beam
K_0	1380 kNm^2	610 kNm^2
K_1	276 (20%)	30.5 (5%)
K_2	6.9 (0.5%)	-
K_3	-6.9 (0.5%)	-

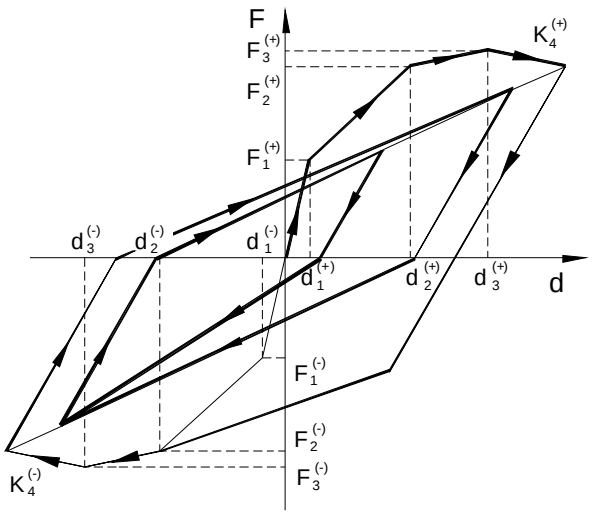

Figure 15: Typical load-displacement curve (tetra-linear Takeda's model).

Based on these values obtained performing a fitting of the unloading stiffness parameters in an identical manner to that used in the tri-linear model, the use of the tetra-linear Takeda's model allowed obtaining the load-displacement curve illustrated in Figure 16.

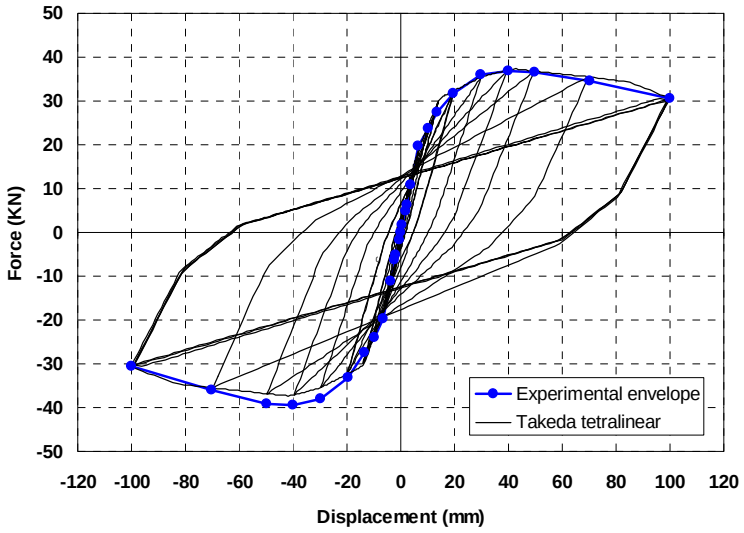

Figure 16: Load-displacement curve (tetra-linear Takeda's model).

From the analysis of Figure 16, it is clear that the tetra-linear model is the one that simulates the experimental results in the best way. The possibility of introducing a softening regime allowed simulating the stiffness degradation that occurs for large lateral displacements of the frame and provides a progressive development of the hysteretic cycles.

Thus, this fourth model allows surpassing the limitations associated with the continuous increase of strength with increasing displacement, characteristic of the former three models.
The fiber model (FM) is another methodology that can be used to analyze nonlinearity behaviour and is based on the discretization of a section in elements or fibers that are associated to each material with axial deformation only (Fig 17). Thus, in this methodology a global curve is not defined for a section (the envelope curve), but with the constitutive laws of the materials that compose the section (Deng et al. [9]). The envelope law is then determined through a rotation/moment increasing. The software fiber model is based on the following limitations: the section shape remains unchanged in the deformation process though remains perpendicular to neutral axis and, therefore, reinforcement slipping is not considered. One of the great advantages of this method consists on the possibility of localizing the position of neutral axis.

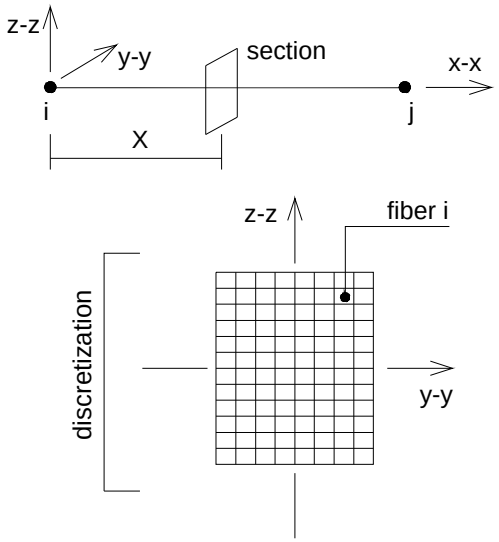

Figure 17: Fiber model and section discretization.

In the FM the state of each fiber is evaluated through the corresponding axial deformations due to axial force and also fiber flexion deformations. The axial force and the flexion moment of the section are then calculated from the tension level in each fiber. The section properties insuring nonlinear behaviour are defined through a tension-extension relation (stress-strain) of the fibers that constitutes the all section.
The FM is more efficient because it allows computing the section moment-rotation constitutive law (that is later used in the global M-R-P or M-ϕ-P curves) but with a more laborious numerical effort because it implies a section subdivision into fibers that are associated with the elementary behaviours previously defined.

The materials constitutive laws have to rigorously reproduce the real behaviour in order to get a reasonable section envelope of the member and structure that is intended to study. The experimental steel traction test allows characterizing with sufficient rigorousness its mechanical behaviour.

However the concrete uniaxial compression test does not allow characterizing this material conveniently due to lateral reinforcement that increases the confinement significantly and therefore the resistant capacity.
In this in case an adjustment process must be carry out to set the parameters that reproduce the experimental behaviour. In this context, the Magenotto-Pinto steel model was used in this study. This is an especially well known bilinear model used for this type of analysis and the behaviour associated with this model is represented in Figure 18. The constitutive law is asymptotically close to the steel envelope in each cycle of the hysteretic curve. The transition between two asymptotes corresponds to the regions of discharge and as the deformation increases in that direction a softer curvature transition is obtained.

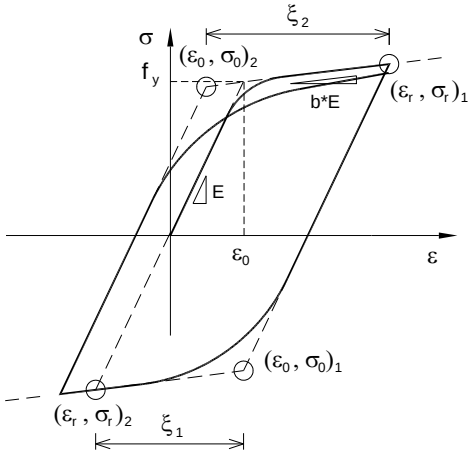

Figure 18: Magenotto-Pinto model (steel).

This model is defined by two parts: an ascending part represented by a second order equation and a linear decreasing part associated with the load release. The ascending part is defined by the following equation:

$$f_s' = b \cdot \varepsilon' + \frac{(1-b) \cdot \varepsilon'}{\left(1+\varepsilon'^{R}\right)^{1/R}} \tag{4}$$

with

$$\varepsilon' = \frac{\varepsilon - \varepsilon_r}{\varepsilon_0 - \varepsilon_r} \tag{5}$$

$$f_s' = \frac{f_s - f_r}{f_0 - f_r} \tag{6}$$

$$R = R_0 - \frac{a_1 \cdot \xi}{a_2 + \xi} \tag{7}$$

In these expressions: ε is the longitudinal steel fibber strain, f'_s the fibber steel stress, (ε_r , f_r) the discharge starting point, (ε_0 , f_0) the asymptotic intersection point that defines the charge-discharge path, b a stiffness reduction factor; R_0, a_1, and a_2 are constant values (R_0 = 20, a_1 = 18.5 and a_2 = 0.15) and ξ the variation between the maximum deformation value in the charge and discharge path directions.
The model used to simulate the concrete behaviour was developed by Kent and Park [10] and is represented in Figure 19. In this model the tension concrete resistance contribution is not considered and the confinement due to existence of lateral reinforcement can be simulated.

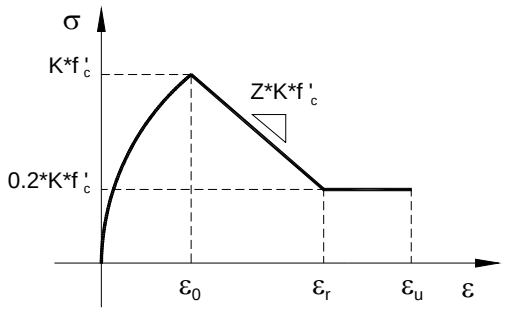

Figure 19: Kent and Park model (concrete).

The constitutive model consists of three parts (Figure 19): an ascending second order equation, a linear descending part and a constant stress part. The ascending part is defined by the following equation:

$$f_c = k \cdot f'_c \cdot \left[\frac{2 \cdot \varepsilon_c}{\varepsilon_0 \cdot k} - \left(\frac{\varepsilon_c}{\varepsilon_0 \cdot k} \right)^2 \right] \tag{8}$$

valid for $\varepsilon_c \leq k \cdot \varepsilon_0$, where ε_c is the longitudinal concrete strain, f'_c the resistant concrete compression capacity, ε_0 the unconfined concrete strain and k the confinement coefficient. (k=1 for the unconfined concrete and ε_0=0.002).
For stresses higher than the yielding stress the descendent part is approximately linear and can be represented by the following equation:

$$f_c = k \cdot f'_c \cdot \left[1 - Z_m \left(\varepsilon_c - k \cdot \varepsilon_0 \right) \right] \tag{9}$$

$$f'_s = \frac{f_s - f_r}{f_0 - f_r} \tag{10}$$

$$R = R_0 - \frac{a_1 \cdot \xi}{a_2 + \xi} \tag{11}$$

This equation is valid for $\varepsilon_c > k \cdot \varepsilon_0$ with $f_c \geq 0.2 \cdot k \cdot f'_c$ and Z_m is the stress ratio in the descending part of the confined concrete. It is assumed that the unconfined concrete strain reduces to zero when $\varepsilon = 0.0035$.
The first step for the application of this method involves the characterization of the materials and subsequent discretization of sections.

The characteristics of the materials used in this work are in accordance with those that were used in the experimental procedure, except for the concrete confinement for which successive attempts were made to obtain plausible confinement value. The concrete cover does not present confinement and the used values translate this characteristic.
This model has the advantage of tracing the section moment-rotation relationship, the monitoring of the neutral axis position and the possibility to establish the axial force level in each fiber. If some sections are used, it is also possible to determine the extension of the plastic hinge zone. Figure 20 shows the discretization used in the critical sections of the RC elements.

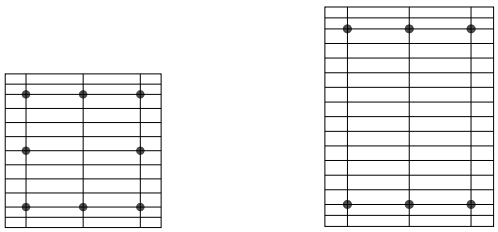

a) column b) beam

Figure 20: Discretization of the RC sections.

It was verified that a load application device was used in the experimental model that constrained the top rotation of the columns. This condition was used in the numerical model to simulate the experimental model conveniently. In fact, the analysis of the damage in sections of the bar elements (columns and beam) allows verifying that the experimental device limits the beam deformation during the experiment, and the behaviour of this element can remain in a linear elastic regimen. In this case it can be considered that the nonlinear behaviour is concentrated in the extreme sections of the two columns.
After attributing these sections to each frame element, a nonlinear analysis was carried out and the obtained results are shown in Figure 21.
It is verified that the envelope obtained through this methodology presents a good approximation to the experimental model, also in the development of the hysteretic curves that present a more real evolution with gradual variations of the load-discharge cycles. Knowing the limitations associated to the constitutive laws and also that this model works well for moderate lateral displacements, its use can be very advantageous when a further section analysis is intended.

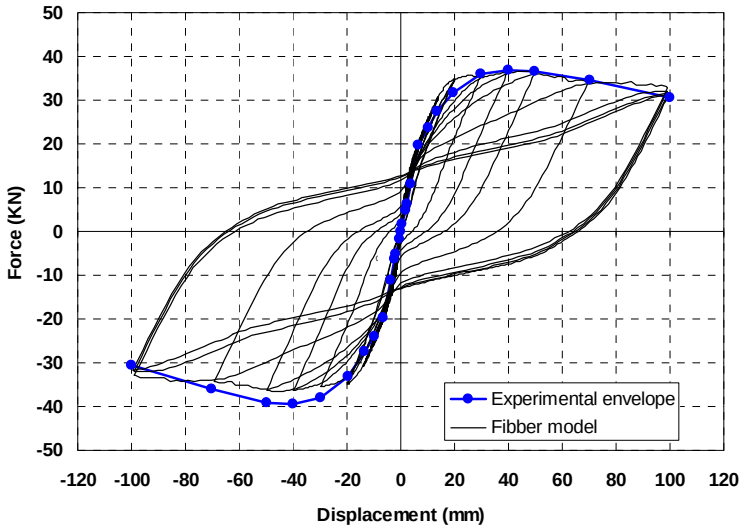

Figure 21: Load-displacement curve (fiber model).

To better understand the performance of each model, a comparison was elaborated (Figure 22) of the cumulative deformation energy stored in the structure. The energy curve obtained during the experimental program at LNEC (curve 5 in Figure 22) was scanned from that presented originally in [1].

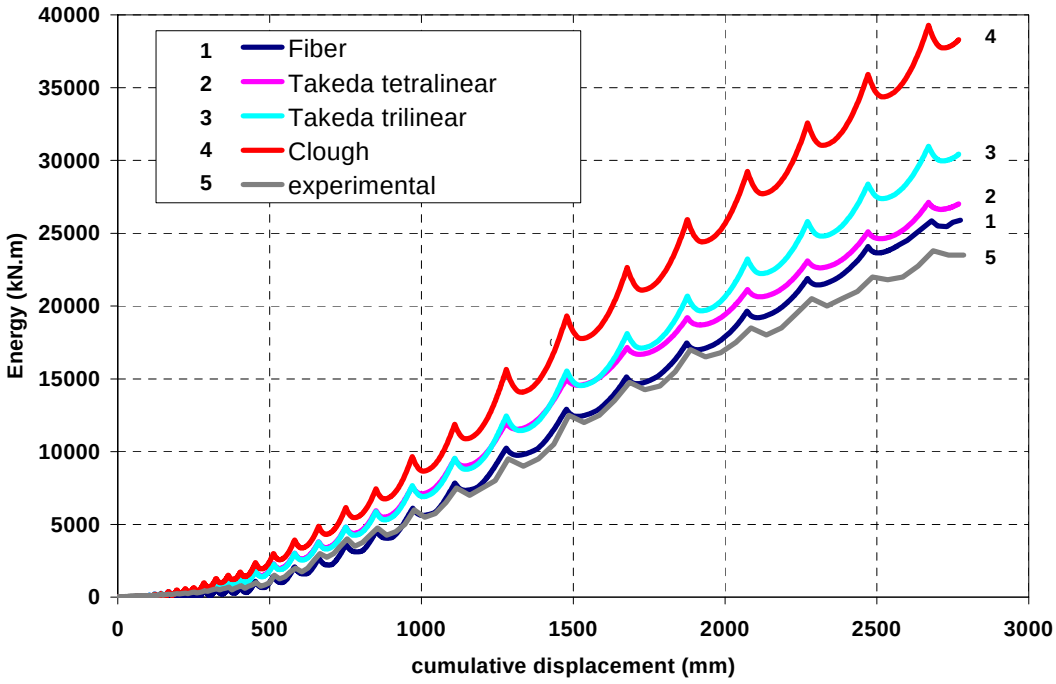

Figure 22: Cumulative energy comparison.

At this stage one should bear in mind that all the structural performance and inherent structural behaviour is a direct consequence of internal energy adaptations and transfers in response to the external energy or external actions on the structure.

Therefore, the energy representation in Figure 22 allows clarifying any doubts as well as assess accuracy and even any uncertainties of the models used, as measured by the closeness of each energy diagram to the one corresponding to the experimental results obtained at LNEC.
It is evident that all the models have higher values compared to the experimental model. It is verified that the Clough's bilinear model is the worst approach (higher accumulated energy than the one of the experimental setup) as compared to the experimental model, situation expected since this model does not conveniently represent the behaviour of the frame elements.
The remaining models are very close to the experimental model, being the fiber model and the tetra-linear Takeda's model those that better represent the structure behaviour. The fiber model is the more elaborated model and the results obtained emphasize a good approximation to the experimental model; however, the use of this methodology requires a deep knowledge of the involved materials and the refining of the parameters (corresponding to such good fitting) can be significantly time consuming.

4 Numerical model of RC infill frame

In this chapter a simplified model to analyse an infill masonry frame is exposed, and is detailed a computed example based on the previous bare frame geometry that was tested at the LNEC facilities [1]. As mentioned at the beginning of the paper a regular brick wall was constructed into the bare frame and then the same experimental analysis was carried out.

Although the masonry construction can perform a variety of functions such as structural resistance, often this capability is not consider in the building design namely when a seismic event is involved. If a wall and the envelope frame can be considered to act as a single composite component, then an initial structural resistant increase can be expected (Maganes and Calvi [11] ; Fardis and Panagiotakos [12]). At this point it is necessary to compute the proportion of the load acting on the infill and the behaviour evolution, to understand the global performance of the structure.
One of the more important aspects related with the infill frame resistance is the bond between the brick wall and the columns and beams, to allow the development of the required contact forces. The LNEC experimental procedure was prepared to study this effect on the global behaviour of the infill frame, and several infill frames were analysed. However in the present study it was decided to analyse only an unbounded infill frame because: (i) a simplified analysis is required; (ii) the widespread commercial design software cannot consider this phenomena; (iii) also, this is a more realistic construction process.

Although this is important information regarding the behaviour of infill RC frames, the nonlinear simplified approach used in this study requires a basic model for the infill panel to allow adding this element to the structural model (Brokken and Bertero [13]). Basically, the infill structure behaviour can be compared with a frame filled with diagonal struts (Haach et al. [14]) that simulate the walls (Figure 23a).

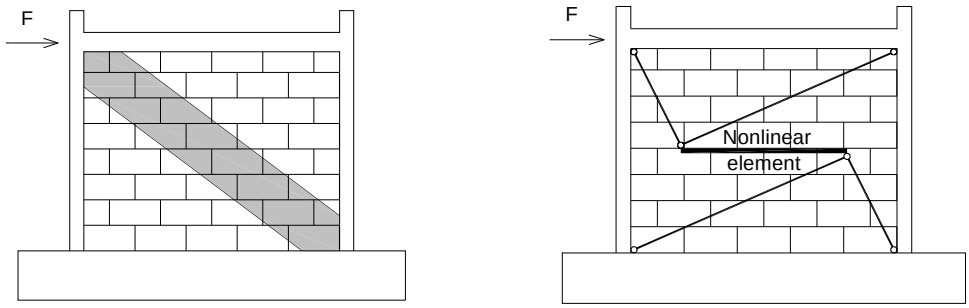

a) equivalent diagonal strut b) interaction model

Figure 23: Idealized force-displacement relationship.

This methodology allows simulating, by a simplified nonlinear element, the global infill RC frame behaviour without increasing the total structural degrees of freedom. On the other hand, this simplification presents some important limitations such as: only suitable for full infill panels; does not consider the length of contact of the infill panel with the elements that confine it; does not take into account the infill rupture mode that significantly modifies the distribution of efforts in the frame; is based on the principle that only the axial strut capacity simulates the wall stiffness contribution; the different values pointed by several authors with respect to the strut width are very different, having this parameter to be surveyed for each type of masonry.

A more sophisticated model, based on the model of the double equivalent struts but with significant improvements relatively to the classic model, can be used. In this case to represent the masonry panel four rigid struts with linear elastic behaviour are used that give support to a fifth central element where the hysteretic nonlinear behaviour of the panel is concentrated as shown in Figure 23b. This model was used in this study with the advantage of introducing the interaction between the two struts that in the classical approach act independently. The nonlinear behaviour of the masonry infill is concentrated in the central element of the macro-model and is characterized by universal rules that reproduce the load history and depend on the law of material behaviour imposed, as those described for the bare frame.

The geometric and mechanical characteristics of this element must reproduce the real behaviour of the filling walls. In Figure 24a is shown a normally used force-displacement relationship for the infill equivalent element. In this study a numerical fitting was used to define a realistic nonlinear element envelope and although there was this need to assume some parameters, the proposed model was able to simulate closely the experimental behaviour of the infill RC frame as it will be proved later in this section. The global behaviour of an infill RC frame can also be idealized as a multi-linear force-displacement relation that defines the envelope of the cyclic loading or of a pushover analysis (Barros and Almeida [15]; Dolsek and Fajfar [16]), and a typical idealized force-displacement relation is shown in Figure 24b.

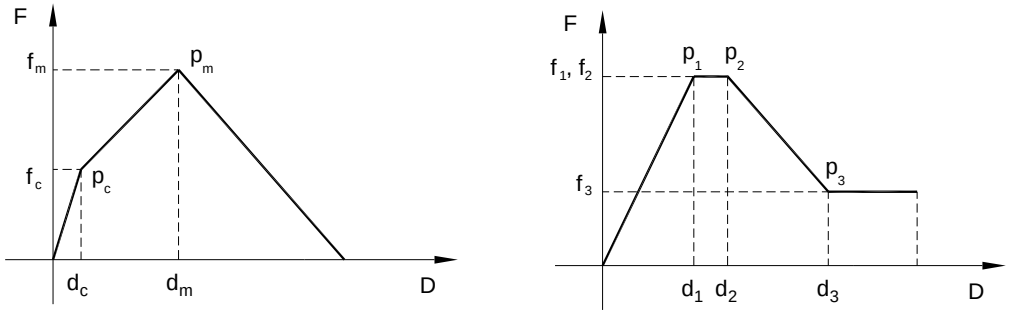

a) Nonlinear equivalent element b) Infill RC frame envelope

Figure 24: Idealized force-displacement relationship.

In this latter approach the envelope is divided into four branches: an initial equivalent linear part that simulates the monolithic elastic and after cracking behaviour of the infill RC frame; a second part normally small due to lack of ductility of infill frames that represents yielding (between P1 and P2); a third part governed by the infill in which a degradation in observed until P3 is reached; the last part, after P3, is related with the infill collapse and when only the RC frame oppose the horizontal loads.

It is obvious that there is an increase in stiffness and strength of the infill RC frame before reaching the deformation demand capacity of the infill masonry as shown by the force-displacement envelopes in Figure 25.

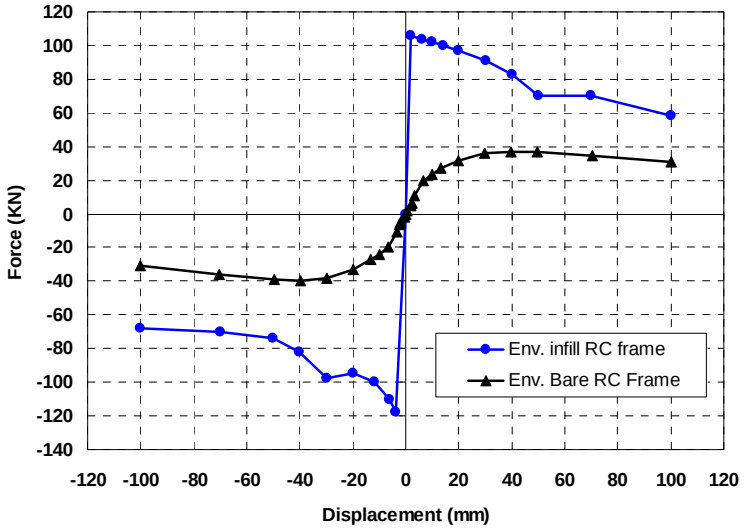

Figure 25: Infill and bare RC frame envelopes.

The results of the numerical analysis (finished after setting the nonlinear equivalent strut parameters) are shown in Figure 26.

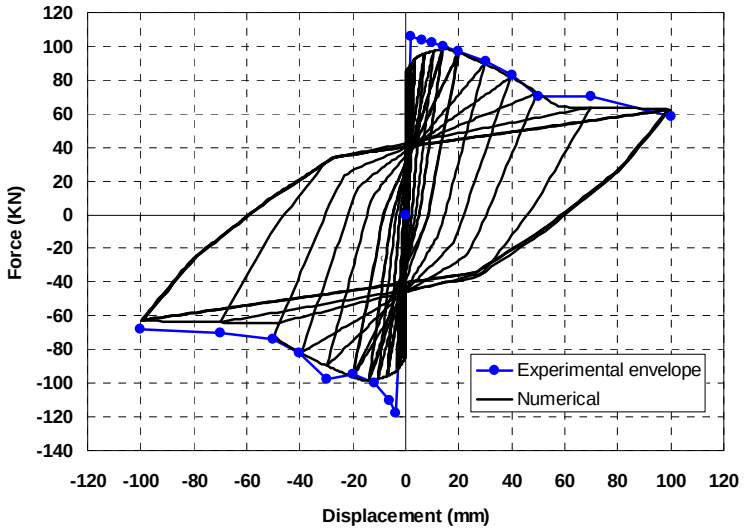

Figure 26: Global force-displacement cyclic relationship for the infill RC frame.

In this representation it is clear that the simplified model suits notably well the infill RC frame experimental envelope. A slight deviation of the numerical values from the experimental results is evident at the beginning of the hysteretic envelope, with an error less than 5% that is acceptable for any engineering purposes. At the last cycles there is also some slight disparity between the numerical and the experimental results explained by the large incursion into the nonlinear regime that is very difficult to simulate with such limited models.

However, although satisfying the cyclic behaviour with similar cyclic shapes, it is verified that the computational models do not have the necessary strength degradation capability to ensure a correct representation of the hysteretic behaviour. This evidence allows to conclude that instead of this simplified analysis through this computational commercial package MIDAS [2], it is may be more convenient to perform a continuous increased loading analysis (a pushover analysis) in which the final result reflects the envelope of the cyclic analysis.
Further studies are being made to evaluate new simplified models in order to improve the presented numerical results. The conclusion about such envelope analysis indicates a need for a parametric study of infill RC frames through a pushover analysis that will constitute further developments of the present work.

5 Conclusions

This article presented a study about simplified nonlinear material models based on restricted inelastic region behaviour of structural elements, that further are used to simulate cyclic performance of a bare and an infill frame. In this simplified approach the original structural member nonlinear section is modelled by a nonlinear hinge with an equivalent moment-curvature relationship. The mathematical model was validated by comparing the nonlinear simplified analysis results with the experimental results.

The first obvious conclusion, based on the numerical results of this study, allows to verify that increasing the complexity of the inelastic hinge constitutive law implies a better global nonlinear fitting of the analyzed frames behaviour. So the numerical results show that it is possible to accurately reproduce the experimental results if a correct computational model is selected. The use of more complex and more rigorous models does not necessarily mean a significant increase of the quality of the obtained results. The involved parameters in the definition of the more complex models (fiber model) contribute to a more delicate calibration procedure, implying resources consumption that cannot lead to a qualitative enhancement of the results comparatively to the simplest models for study of the global structure behaviour.
Another important visible aspect in this work is related with the numerical difficulty to represent large incursions in the nonlinear regime as observed in the experimental test. The simplified infill model can be used for envelope analysis but the hysteretic behavior needs a more accurate nonlinear simplified model.

Acknowledgments

This paper reports research developed under the R&D Eurocores Project COVICOCEPAD within the S3T Program, approved independently by European Science Foundation (ESF, Strasbourg), through financial support provided by "FCT - Fundação para a Ciência e a Tecnologia" (Lisbon, Portugal).

References

[1] F. Pires, "Influência das paredes de alvenaria no comportamento de estruturas reticuladas de betão armado sujeitas a acções horizontais", PhD Thesis, LNEC, 1990 (*in Portuguese*).
[2] Midas Inc., Analysis manual: Inelastic time history analysis, Korea, 2004.
[3] M.N. Fardis, T.B. Panagiotakos, "Seismic design and response of bare and masonry-infilled reinforced concrete buildings. Part I: Bare structures", Journal of Earthquake Engineering, Vol. I, No 1, 219-256, 1997.
[4] T. Paulay, M.J.N. Priestley, "Seismic design of reinforced concrete and masonry buildings", John Wiley & Sons Inc., New York, 1992.
[5] M.B. Cesar, D.V. Oliveira, R.C. Barros, "Validação Numérica da Resposta Cíclica Experimental de Pórticos de Betão Armado", 7º Congresso Nacional de Mecânica Experimental – APAET 2008, UTAD, Vila Real, 23-25 Janeiro 2008. ISBN: 978-972-669-851-7, Depósito Legal: PT 269753/08; Eds.: Abílio M.P. de Jesus & Jorge T.Q.S. Pinto; pp. 117-119, Lisboa: APAET, 2008 (*in Portuguese*).
[6] M.B. Cesar, D.V. Oliveira, R.C. Barros, "Cyclic Experimental Response of Reinforced Concrete Frames: validation methodology", Proceedings of the 13th International Conference Mechanika 2008, Paper 119, pp. 1-3, Kaunas, Lithuania, 2008.

[7] M.B. Cesar, D.V. Oliveira, R.C. Barros, "Validação Numérica da Resposta Cíclica Experimental de Pórticos de Betão Armado"; Submitted for publication in the journal *Mecânica Experimental*, pp. 1-13, Lisbon, APAET, 2008 (*in Portuguese*).

[8] J.W. Wallace, "BIAX – A Computer Program for the Analysis of Reinforced Concrete and Reinforced Masonry Sections". Report No. CU/CEE-92/4, Department of Civil Engineering, Clarkson University, Potsdam, New York. 1992.

[9] H. Deng, Y. Chang, D. Lau, S. Ostovari, K. Tsai, "A simplified approach for nonlinear response analysis of composite structural members", International Workshop on Steel and Concrete Composite Constructions, NCREE, Taiwan, 207-216, 2003.

[10] D.C. Kent, T. Park, "Flexural Members with Confined Concrete", Journal of Structural Division, Proceedings of the American Society of Civil Engineers, Vol. 97, No. ST7, 1969-1190, 1975.

[11] G. Maganes, G.M. Calvi, "In-plane seismic response of brick masonry walls", Earthquake Engineering and Structural Dynamics, Vol. 26, 1091-1112, 1997.

[12] M.N. Fardis, T.B. Panagiotakos, "Seismic design and response of bare and mansory-infilled reinforced concrete buildings. Part II: Infilled structures", Journal of Earthquake Enginnering Vol. I, No 3, 475-503, 1997.

[13] S. Brokken, V.V. Bertero, "Studies on effects of infill in seismic resistant RC construction", Report UCB/EERC, University of California, Berkeley, 81-12, 1981.

[14] V.G. Haach, G. Vasconcelos, P.B. Lourenço, "Cyclic behaviour of truss type reinforced concrete masonry walls", SISMICA2007, FEUP and SPES, Porto, Portugal, 2007 (*in Portuguese*).

[15] R.C. Barros, R.F. Almeida, "Pushover Analysis of Asymmetric Three-Dimensional Building Frames", Journal of Civil Engineering and Management, Vol. XI, Nº 1, pp. 3-12, Vilnius, Lithuania, 2005.

[16] M. Dolšek, P. Fajfar, "The effect of masonry infills on the seismic response of a four-storey reinforced concrete frame – a deterministic assessment", Engineering Structures, Elsevier Ltd., 2008.